Visible light harvesting Alkyne hydrosilylation mediated by pincer platinum complexes

*Laura Ibáñez-Ibáñez,[a] Ariadna Lázaro[b], Carmen Mejuto,[a] Margarita Crespo,[c] Cristian Vicent,[d] Laura Rodríguez,[*b] and Jose A. Mata[*a]*

[a]Institute of Advanced Materials (INAM), Centro de Innovación en Química Avanzada (ORFEO-CINQA), Universitat Jaume I, Avda. Sos Baynat s/n, 12071, Castellón (Spain). E-mail: jmata@uji.es
[b]Departament de Química Inorgànica i Orgànica, Secció de Química Inorgànica, Universitat de Barcelona, E-08028 Barcelona (Spain). Institut de Nanociència i Nanotecnologia (IN2UB), Universitat de Barcelona, 08028, Barcelona (Spain).
[c]Departament de Química Inorgànica i Orgànica, Secció de Química Inorgànica, Universitat de Barcelona, E-08028 Barcelona (Spain). Institut de Biomedicina de la Universitat de Barcelona (IBUB), 08028, Barcelona (Spain).
[d]Serveis Centrals d'Instrumentació Científica (SCIC). Universitat Jaume I, Avda. Sos Baynat s/n, 12071, Castellón (Spain).

Keywords:

Photocatalysis, hydrosilylation, platinum, mechanisms, HAT

ABSTRACT

In this manuscript we assess the catalytic properties of pincer platinum complexes in alkyne hydrosilylation either under photo or thermal conditions. The visible light-induced hydrosilylation proved to be more efficient. It can be performed at room temperature and required lower catalyst loadings than that operating under thermal conditions. The platinum complexes play a dual role in photohydrosilylation as serve as a photosensitizer and a catalyst enabling species in bond breaking/forming transformations. In addition, alkyne hydrosilylation is achieved with moderate regio- and stereoselectivity but is enhanced under photocatalytic conditions and in the case of terminal alkynes we have observed the formation of β(Z) products not observable under thermal conditions. Such differences in selectivity constitute an example of stereodivergent catalysis dictated under photochemical or thermal conditions. The selectivity differences are ascribed to a distinctive reaction mechanism for the light- vs thermally-induced process that involve radical or organometallic intermediates, respectively.

1. INTRODUCTION

Hydrosilylation of alkynes constitutes a direct and atom-economical approach for the preparation of vinylsilanes, a family of important synthons in industry as well as organic chemistry.[1–4] The dominant method of choice relies on the activation of a Si-H bond using transition metal catalysts. In particular, platinum catalysts represent the most active systems for hydrosilylation of alkynes.[5–9] Their high activity and the highly sensitive nature of the reaction intermediates is precisely behind the comparatively scarce number of mechanistic investigations of platinum-based systems with respect to their less-active transition metals.[10–12] One of the most widely accepted mechanisms for this transformation was first reported by Chalk and Harrod in 1965.[13] It involves organometallic intermediates and typically initiates via an oxidative addition of the Si-H bond to a Pt(0) alkyne complex, followed by migratory insertion of the alkyne into the metal-hydrogen bond. Subsequent reductive elimination of alkenyl and silyl ligands gives rise to the hydrosilylation products.

Silyl radicals ($R_3Si\cdot$) are also convenient and versatile intermediates able to promote the formation of C-Si bonds by addition into a target molecule bearing alkyne (or alkene) functional groups.[14–18] Visible light-induced photocatalysis has become a powerful tool to produce silyl radicals and it has been exploited extensively in hydrosilylation processes.[19–22] Silyl radicals can be obtained from hydrosilanes and their formation usually requires a photocatalyst, which in its excited state is capable of activating the silane via hydrogen atom transfer (HAT) processes. These $R_3Si\cdot$ intermediates subsequently add to the alkyne (alkene) to produce the more stable silyl radical. A second HAT process involving these silyl radical forms the desired vinylsilanes. In this context, visible light-induced transition metal catalysis constitutes an emerging class of photocatalysis that is receiving considerable attention.[23–28] These photocatalytic systems rely on the use of transition metal complexes able to act simultaneously as both i) photosensitizer and as ii) catalyst in conventional bond breaking/forming processes.

Regarding hydrosilylation reactions, the use of visible light-induced transition metal photocatalysis is relatively scarce. Examples are restricted to the use of polyoxometallates[29] and Mn,[30,31] complexes which in their excited states are able to homolytically activate the Si-H bond in trisubstituted silanes to produce silyl radicals engaged in the efficient hidrosilylation of alkenes and alkynes. Such single-component catalytic systems constitute a novel and underexplored reaction manifold in hydrosilylation chemistry whose exploration aimed at developing improved methods, in particular for platinum, still needs to be undertaken. Photohydrosilylation procedures mediated by Pt are known in industry since three decades ago but detailed mechanistic investigations are negligible.[32] Other photo-triggerable hydrosilylation reactions mediated by platinum have been reported using complexes with O-donor ligands (β-diketonate or oxalate),[33–41] or aminocarbene and carbene ligands.[42,43] It was reported that irradiation promotes peripheral ligand releasing to afford a highly active homogenous species that triggers hydrosilylation via classical Chalk-Harrod mechanisms rather than silyl radicals. Photoinduced hydrosilylation is also promoted by the platinum catalyst (η^5-$C_5H_4CH_3$)$Pt^{IV}(CH_3)_3$,[44,45] which anticipated the potential of Pt complexes as photoinitiators in various free-radical-mediated transformations. Pincer-type NCN Pt complexes might be useful for this purpose because they combine photoactive character along with their inherent catalytic versatility.[46] Herein, a room temperature platinum/blue light hydrosilylation of internal and terminal alkynes is reported using single-component catalytic systems based on pincer (NCN)Pt complexes (Figure 1).

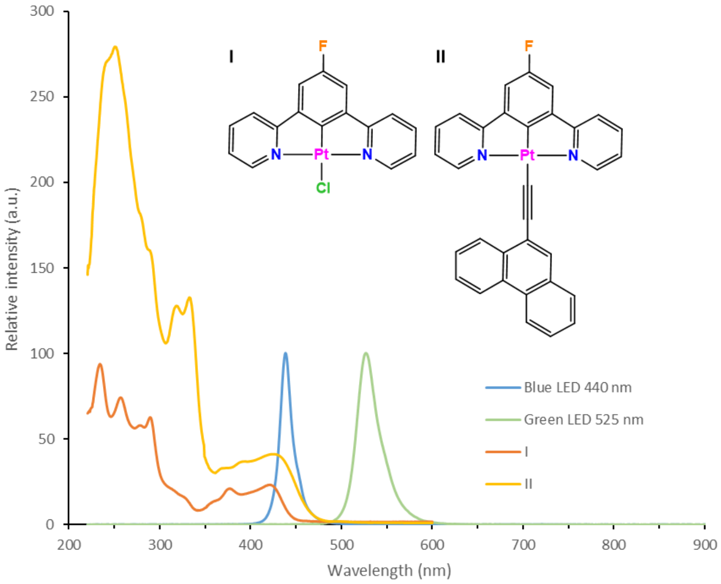

Figure 1 UV-Vis absorption spectra of complexes **I** and **II** in CH_2Cl_2 (5.0 x 10^{-5} M) overlaid with emission spectra of blue and green Kessil PR160L LED lamps.

2. EXPERIMENTAL SECTION

All manipulations were conducted with a standard Schlenk line under nitrogen atmosphere. Alkynes and silanes were purchased from commercial suppliers and used without further purification. Anhydrous solvents were dried using a Solvent Purification System (SPS M BRAUN) or purchased from commercial suppliers degassed and stored over molecular sieves. Solvents used in catalytic experiments were deoxygenated using the freeze-pump-thaw methodology and kept under an atmosphere of nitrogen.

Nuclear magnetic resonance (**NMR**) spectra were recorded on Bruker spectrometers operating at 400 MHz (^1H NMR) and referenced to $SiMe_4$ (δ in ppm and J in Hertz). NMR spectra were recorded at room temperature with the appropriate deuterated solvent. ESI-MS studies were conducted on a SYNAPT HDMS QTOF instrument with an orthogonal Z-spray-electrospray interface (Waters, Manchester, UK) operating in the resolution mode. The drying and cone gas was nitrogen set to flow rates of 600 and 100 L/h, respectively. A capillary voltage of 2.5 kV was used in the positive ESI(+) scan mode. The cone voltage was kept to a low value (typically Uc = 5−30 V) to control the extent of fragmentation in the source region. Chemical identification of the Pt-containing species was facilitated by the characteristic isotopic pattern at natural abundance of Pt and it was carried out by comparison of the isotope experimental and theoretical patterns using the MassLynx 4.2. Typically, methanol solutions of **I** and **II** were stirred under catalytic conditions and aliquots were extracted at spaced time intervals, diluted with methanol to a final concentration of 1 x 10^{-6} M (based on the initial Pt concentration) and directly introduced to the mass spectrometer. UV−Vis spectra were recorded in CH_2Cl_2 with a Cary 100 scan 388 Varian UV spectrometer. Emission and excitation spectra were recorded in a Horiba Jobin-Yvon SPEX Nanolog-TM spectrofluorometer at 298 K using 5×10^{-5} M solutions.

2.1. Catalytic hydrosilylation under thermal conditions

General procedure: Alkyne (0.3 mmol, 1.0 eq.), silane (0.35 mmol, 1.2 eq.), complex **I** or **II** (0.7 mol%), 1,3,5-trimethoxybenzene (0.1 mmol, 0.33 eq., used as an internal standard), deoxygenated toluene (2.0 mL), and a PTFE-coated magnetic bar were placed in a 12 mL Schlenk flask closed with a septum. The solution was stirred at 80 °C in an oil bath for 7 hours. At selected times, 100 mL aliquots were extracted and analysed by GC-FID to monitor the reaction evolution. When the reaction was completed, the solution was evaporated to dryness, redissolved in $CDCl_3$ and analysed by ^1H NMR spectroscopy. Selectivity was determined by integration of selected peaks (vinylic protons) vs 1,3,5-trimethoxybenzene.

2.2. Photohydrosilylation

General procedure: Alkyne (0.3 mmol, 1.0 eq.), silane (0.35 mmol, 1.2 eq.), selected catalyst (0.25 mol%), 1,3,5-trimethoxybenzene (0.1 mmol, 0.33 eq., used as an internal standard), deoxygenated toluene (2.0 mL), and a PTFE-coated magnetic bar were placed in a 12 mL Schlenk flask closed with a septum. The photocatalytic reactions were carried out using 45W Kessil PR160L blue LEDs (λ= 440 nm) lamps placed at the distance of 5 cm of the centre of the Schlenk (intensity of 172 mW/cm^2) at room temperature for the appropriate time. At selected times, 100 mL aliquots were extracted and analysed by GC-FID to monitor the reaction evolution. When the reaction was completed, the solution was evaporated to dryness, redissolved in $CDCl_3$ and analysed by ^1H NMR spectroscopy. Selectivity was determined by integration of selected peaks (vinylic protons) vs 1,3,5-trimethoxybenzene.

3. RESULTS AND DISCUSSION

The d^8 platinum (II) complexes containing polypyridyl ligands are relevant in photochemistry since modulation of the photophysical properties is easily achieved by subtle changes in ligand design.[47–50] In this work, we have selected as representative examples two platinum complexes containing a NCN tridentate ligands combined with a Cl or an alkynyl monodentate ligand previously described by us(Figure 1).[46] NCN coordination is achieved by C-H activation under acidic media using K_2PtCl_4 under microwave irradiation. The absorption photophysical properties are characterized by the presence of an intense band in the higher energy region (270 - 350 nm) attributed to $^1\pi$- π^* transition of the NCN ligand and less intensity bands in the lower energy region (350 – 450 nm) which correspond to mixed charge-transfer ligand-centred character transitions.[51–53] These latter bands overlaid with the emission spectra of blue lamp (440 nm) used in the photocatalytic studies as required according to the first law of photochemistry (Grotthuss-Draper law) which states that light must be absorbed by a chemical substance to perform a photochemical transformation.[54,55] The emission properties show the presence of two bands assigned to the $^3\pi$-π^* transition from the NCN ligand mixed with ^{3}MLCT/^{3}ILCT (Figure S5).[56–58]

Interested in developing applications of platinum complexes we assess the catalytic properties of platinum complexes harvested with visible light. In a first set of experiments, we evaluated the catalytic activity of the platinum complexes under thermal and photocatalytic conditions (Table 1). We selected 1-phenyl-1-butyne and dimethylphenylsilane as model substrates due to their stability, availability and well-documented transformations. Initially we carried out the hydrosilylation of alkynes under mild thermal conditions (40 °C) but the reaction did not proceed independent of the platinum complex used (Table 1, entries 2&3). When increasing the temperature to 80 °C, complexes **I** and **II** become efficient catalysts in hydrosilylation of alkynes. For instance, when using a catalyst loading of 0.7 mol%, a quantitative yield is obtained in only 7 h (Table 1, entries 6&7). Product selectivity shows slight differences for complexes **I** and **II** affording an α/β product distribution of 71/29 and 63/37 respectively after 7h. We have observed that the α/β ratio is independent of reaction time.

Then, we assessed the photocatalytic properties of platinum complexes using visible light. Without adding a catalyst, no reaction was observed in the 20–80 °C range with blue light irradiation (Table 1, entries 8&9) indicating that irradiation itself is not sufficient to initiate this process. To our delight, we observed a quantitative yield in the hydrosilylation of 1-phenyl-1-butyne with dimethylphenylsilane using blue light (440 nm) either with complex **I** or **II** at room temperature in only 2h (Table 1, entries 10&11). When changing the irradiation lamp to green light (525 nm) we observed that the reaction proceeds but with lower yield (4h, 42%). These results agree with the photochemical studies of complexes **I** and **II**. There is a significant overlap between the lower energy bands (region 350 – 450 nm) of complexes **I** and **II** with the blue lamp but almost insignificant in the case of green lamp (Figure 1). Interestingly, the photocatalytic hydrosilylation provides an increased selectivity. With both platinum complexes, the α/β product distribution is ca. 80/20 favouring the formation of the α product whereas ca. 65/35 distributions were observed for the thermal reaction (Table 1, entries 4-7 vs 10-14). Despite the moderate regioselectivity, this constitutes a rare example of regiodivergent catalysis achieved photochemically.[31,59] We assessed the catalyst loading effect in photohydrosilylation using complex **II** (Figure 2a). Variation of catalyst loading from 0.7 – 0.01 mol% vs. alkyne evidence a clear decrease in activity, yet the photohydrosilylation reaction still proceeds when using parts-per-million (ppm) level catalyst loading. For instance, at 100 ppm a 75% yield is obtained in 24h at room temperature (TOF = 312 h^{-1}). We established the order in catalyst using variable time normalization analysis (VTNA).[60] The results suggest an order in catalyst of 1 for the photohydrosilylation reaction using complex **II**, indicating that the reaction rate is linearly proportional to the amount of complex (Figure S8). Light intensity is an important factor that directly influences the reaction rate. However, it is barely evaluated in photocatalysis most probably because is completely dependent of experimental set-up, lamps, and reactor design. In here, we have evaluated the light intensity effect in photohydrosilylation using complex **II** (Figure 2b). The results show a dependence of light intensity vs. activity. We have not observed saturation, but we are very close as the monitoring profiles almost overlapped at high intensities (172 and 127 mW/cm^2) using a catalyst loading of 0.25 mol%. We are in a regime where the effect of light intensity is proportionally linear as evidenced by the representation of reaction rate constant vs. light intensity. These experiments confirm that we do not have losses by light intensification. We have disclosed that a catalyst loading of 0.25 mol% and a light intensity of 172 mW/cm^2 (at 5 cm) are the appropriate parameters to achieve the maximum efficiency in photohydrosilylation of alkynes.

Table 1. Thermal and Photocatalytic hydrosilylation results under various conditions

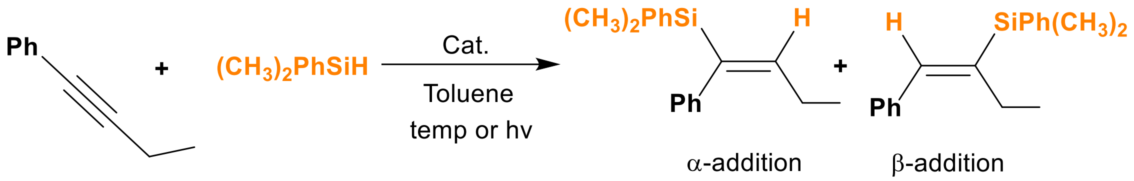

Entry	**Cat. (mol%)**	**Temp (°C)**	**hν λ (nm)**	**Time** (h)	**Yield** (%)[a]	**Selectivity** (%)[a] (α/β)
1	-	80	-	7	0	-
2	**I** (0.7)	40	-	7	0	-
3	**II** (0.7)	40	-	7	0	-
4	**I** (0.7)	80	-	3	34	70/30
5	**II** (0.7)	80	-	3	85	62/38
6	**I** (0.7)	80	-	7	97	71/29
7	**II** (0.7)	80	-	7	98	63/37
8	-	r.t.	440 (blue)	4	0	-
9	-	80	440	4	0	-
10	**I** (0.7)	r.t.	440	2	99	81/19
11	**II** (0.7)	r.t.	440	2	98	81/19
12	**II** (0.7)	r.t.	525 (green)	4	42	80/20
13	**I** (0.25)	r.t.	440	4	98	81/19
14	**II** (0.25)	r.t.	440	4	99	81/19

Reaction conditions: 1-phenyl-1-butyne (0.3 mmol), dimethylphenylsilane (0.35 mmol), toluene (2.0 mL), 45W Kessil PR160L LEDs used for experiments under blue light irradiation (440 nm, 172 mW/cm^2 located at 5 cm). Yields and regioselectivity (α/β) were determined by ^{1}H NMR spectroscopy using 1,3,5-trimethoxybenzene (TMB) as an internal standard.

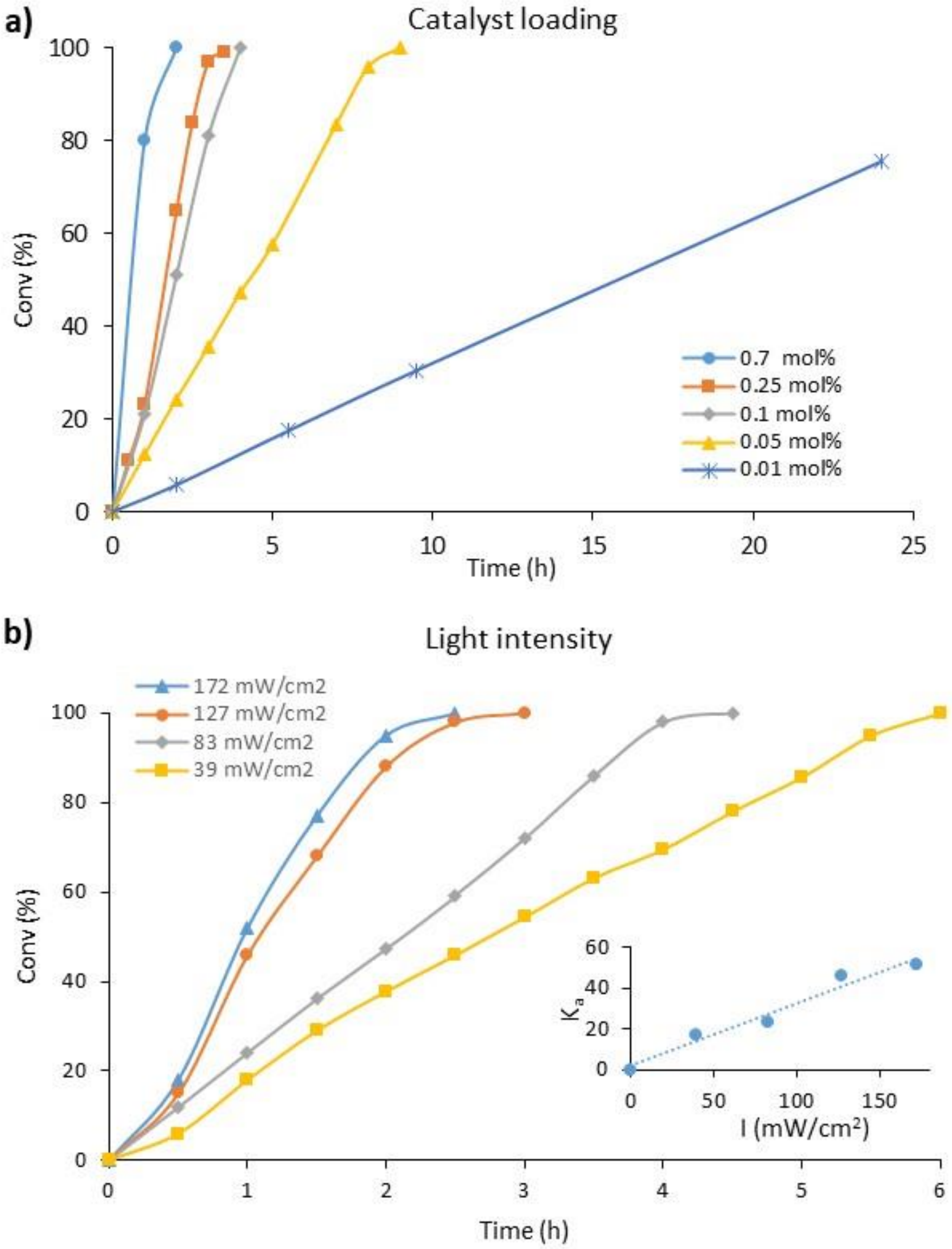

Figure 2 a) Catalyst loading effect. Reaction conditions: 1-phenyl-1-butyne (0.3 mmol), triethylsilane (0.35 mmol), toluene (2.0 mL), complex **II** (0.7 – 0.01 mol%), 25 °C and blue light (440 nm, 172 mW/cm^2 located at 5 cm). b) Lamp intensity effect. Reaction conditions: 1-phenyl-1-butyne (0.3 mmol), triethylsilane (0.35 mmol), toluene (2.0 mL), complex **II** (0.25 mol%), 25 °C and blue light (440 nm, at different intensities measured at 5 cm). Inset: reaction rate constant vs. light intensity. Conversions determined by GC-FID using TMB as an internal standard.

3.1 Hydrosilylation of internal alkynes

Once stablished the optimization of reaction conditions we explore the scope of hydrosilylation. We use different internal alkynes and different silanes under thermal and photocatalytic conditions using complexes **I** and **II** (Table 2). Both complexes are efficient catalysts in hydrosilylation either under thermal or photocatalytic conditions affording quantitative yields. The photocatalytic hydrosilylation is more efficient as it requires i) lower catalyst loadings (0.25 vs. 0.7 mol%), ii) shorter reaction times (4 vs 7h) and iii) lower reaction temperatures (25 vs 80 °C) to achieve complete conversion. A similar observation was highlighted by Marchi and co-workers in terms of energy and time saving for the photo-activated hydrosilylation employing $Pt^{II}(acac)_2$ as catalyst.[40] We have observed a complete selectivity towards the formation of the E isomers with preferential α over β addition products as evidenced by ^1H NMR spectra of final reaction crudes. In addition, higher selectivity is found for photocatalytic hydrosilylation in all cases.

Table 2. Thermal and photocatalytic hydrosilylation of Internal alkynes

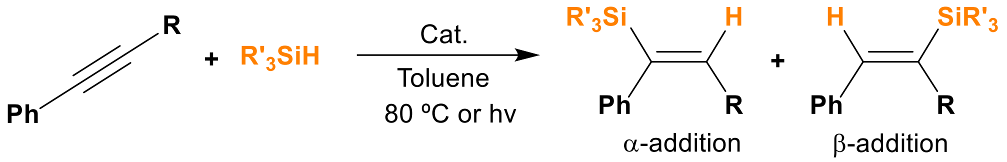

Entry	Cat.	R	Silane	Temp (°C)	hν λ (nm)	Time (h)	Yield (%)	Selectivity (%) α/β
1	**I**	Et	Et_3SiH	r.t.	440	4	95	84/16
2	**II**	"	"	r.t.	440	4	98	84/16
3	**I**	"	"	80	-	7	92	78/22
4	**II**	"	"	80	-	7	92	79/21
5	**I**	*n*Pr	"	r.t.	440	4	95	83/17
6	**II**	"	"	r.t.	440	4	96	83/17
7	**I**	"	"	80	-	4	96	78/22
8	**II**	"	"	80	-	4	98	79/21
9	**I**	Me	"	r.t.	440	4	72	86/14
10	**II**	"	"	r.t.	440	4	91	86/14
11	**I**	"	"	80	-	7	96	81/19
12	**II**	"	"	80	-	7	98	80/20
13	**I**	"	$PhMe_2SiH$	r.t.	440	4	97	72/28
14	**II**	"	"	r.t.	440	4	99	65/35
15	**I**	"	"	80	-	7	96	58/42
16	**II**	"	"	80	-	7	99	63/37
17	**I**	*n*Pr	"	r.t.	440	4	95	82/18
18	**II**	"	"	r.t.	440	4	99	80/20
19	**I**	"	"	80	-	7	97	76/24
20	**II**	"	"	80	-	7	99	77/23

Reaction conditions: alkyne (0.3 mmol), silane (0.35 mmol), toluene (2.0 mL), 0.7 mol% of catalyst (thermal reactions) or 0.25 mol% (photocatalytic reactions), blue light irradiation (440 nm, 172 mW/cm^2 located at 5 cm). Yields were determined by ^{1}H NMR spectroscopy and regioselectivity (α/β vs. the Ph group) by GC-FID using TMB as an internal standard.

3.2 Hydrosilylation of terminal alkynes

We also turned our attention to the possibility of using terminal alkynes, a more inert substrate in this transformation. We selected phenylacetylene as a representative terminal alkyne. Under thermal conditions, complexes **I** and **II** result active catalysts for this transformation with slightly lower activity as in the case of internal alkynes (Table 3, entries 1 - 4). Complex **II** provides quantitative yields in 8h and under the same conditions, complex **I** affords 79% yield. Selectivity assessment reveal the predominant formation of the β addition product where the $SiMe_2Ph$ fragment is located further afield from the phenyl ring (α/β ratio 35/65 respectively). Regarding stereoselectivity we observe only the formation of the E isomer even at short reaction times. These results suggest that the Z isomer is not formed or that isomerization is a fast process. Under photocatalytic conditions, complexes **I** and **II** produce the hydrosilylation of phenylacetylene but require longer reactions times indicating a lower activity when compared to internal alkynes or even under thermal conditions (Table 3, entries 5 – 8). For instance, quantitative yields are obtained using complex **II** (0.25 mol%) after 18h when the average time was only 4h in the case of internal alkynes. In the case of complex **I**, the situation is even worse, and only 38% yield is obtained under the same conditions. We have observed significative differences in the hydrosilylation of terminal alkynes under photocatalytic conditions for complex **I** or complex **II** that contrast our previous observations using internal alkynes. Interesting is the assessment of selectivity. Regioselectivity is similar under thermal or photocatalytic conditions (β addition product is favoured) but stereoselectivity is significantly different. Under thermal conditions we did not observe the formation of the β-Z product, but under photocatalytic conditions this product is formed in ca. 30% product distribution without optimization. This stereodivergent selectivity highlights the potential of photohydrosilylation as stereodivergent methodology in catalysis and suggests a distinctive reaction mechanism for the light- vs thermally-induced reaction.

Table 3. Hydrosilylation of phenylacetylene

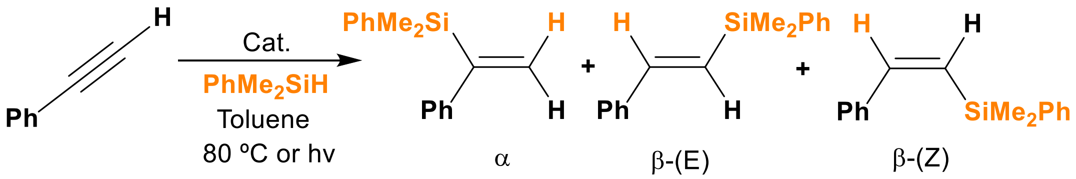

Entry	Cat.	Temp (°C)	hν (nm)	Time (h)	Yield (%)	Selectivity (%) (α/E/Z)
1	**I**	80	-	4	54	34/66/0
2	**II**	80	-	4	75	26/74/0
3	**I**	80	-	8	79	33/67/0
4	**II**	80	-	8	99	33/67/0
5	**I**	r.t.	440	6	24	27/41/32
6	**II**	r.t.	440	6	62	26/42/32
7	**I**	r.t.	440	18	38	24/45/31

8	**II**	r.t.	440	18	99	25/42/33

Reaction conditions: phenylacetylene (0.3 mmol), dimethylphenylsilane (0.35 mmol), toluene (2.0 mL), 0.7 mol% of catalyst (thermal reactions) or 0.25 mol% (photocatalytic reactions), blue light irradiation (440 nm, 172 mW/cm^2 located at 5 cm). Yields, regioselectivity and stereoselectivity were determined by GC-FID and ^{1}H NMR spectroscopy using TMB as an internal standard.

3.3 Mechanistic studies

We attempted to shed some light on the mechanism of both the photocatalytic and thermal hydrosilylation mediated by complexes **I** and **II**. Either the effect of light and the identification of key intermediates is crucial to understand the main and side directions of the studied transformation. The role of light was first assessed by on/off experiments (Figure 3). The hydrosilylation of 1-phenyl-1-butyne with dimethylphenylsilane was monitored with and without light irradiation until completion. The reaction yield increased progressively during the light irradiation periods. In the periods where the light was switched off, the reaction yield remained unchanged. These results confirm that light plays a crucial role throughout the entire course of hydrosilylation and not only in a catalyst activation step.

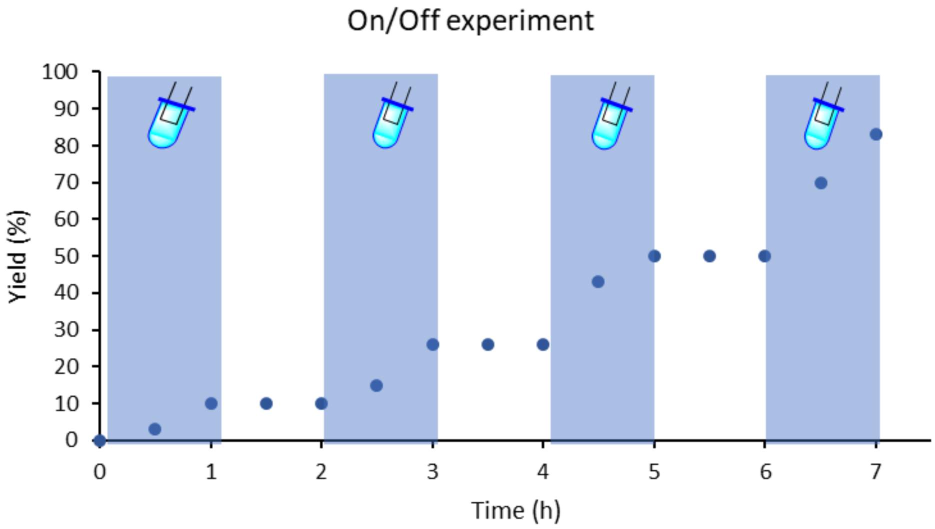

Figure 3 Light influence on photohydrosilylation. Reaction conditions: 1-phenyl-1-butyne (0.3 mmol), dimethylphenylsilane (0.35 mmol), toluene (2.0 mL), complex **II** (0.25 mol%) and blue light irradiation (440 nm, 172 mW/cm^2 located at 5 cm).

Next, the speciation of the catalysts in the presence of light as well as under catalytic conditions was investigated by NMR spectroscopy and Electrospray Ionization Mass Spectrometry (ESI-MS). We typically use a higher catalyst loading than that used in the catalytic runs to facilitate identification of reaction intermediates. Reaction monitoring by ^{1}H NMR analysis allowed us to confirm the advance of the reaction by identifying the initial and final products and provides evidence of catalyst resting state but gives insufficient information about the reaction intermediates formed along the reaction process. However, this limitation is mitigated in combination with ESI-MS, which is one of the most sensitive and powerful techniques to identify reaction intermediates in catalysis,[61–64] including also photochemical transformations.[65]

Reaction monitoring by ^1H NMR spectroscopy in the photohydrosilylation of internal alkynes clearly shows the characteristic signals corresponding to Si-H disappearance and C-H formation of α and β addition products (Figure S31). Interestingly, the ^1H NMR signals of the NCN ligand of **I** are preserved after more than 75% conversion indicating the potential role as resting state of this species. Consistent with ^1H NMR experiments, the ESI-MS monitoring of the catalytic reaction revealed that peaks attributed to **I** and **II** were invariably the dominant species in their respective ESI mass spectra. In both cases, a prominent peak at m/z 444 attributed to the Cl or alkynyl-free complex, namely $[(NCN)Pt]^+$ was observed. The ESI mass spectrum of the catalytic reaction using **II** is exemplified in figure 4b along with that of methanol solutions of **II** for comparative purposes (Figure 4a). A number of Pt-containing species formulated as $[(NCN)Pt]^+$ (m/z 444) and the series of $[(NCN)Pt(alkynyl)+H]^+$ (m/z 645), $[(NCN)Pt(alkynyl)+Na]^+$ (m/z 668) and $[(NCN)Pt(alkynyl)+K]^+$ (m/z 684) cations were common to both spectra; however, a prominent peak at m/z 888 was identified in the catalytic reaction attributed to the $[(NCN)PtPt(NCN)]^+$ dimer. Under catalytic conditions, there was no evidence of oxidative addition of silane to yield neither mono-, dinuclear species or Pt(0) intermediates.[66,67] The origin of the reduced $[(NCN)PtPt(NCN)]^+$ dimer was further investigated upon light irradiation of solutions of **II** in the absence of substrates. We have observed the appearance of low intensity signals in the aromatic region of the ^1H NMR spectrum after 4h that do not evolve for prolonged reaction times (Figure S25). These signals suggest the formation of new species induced by light interaction with the platinum complex. Complementary ESI mass spectra displayed a depletion of the signals of **II** (namely [**II** + cat]$^+$ cat = H, Na and K) and the appearance of a new species formulated as $[(NCN)PtPt(NCN)]^+$ (m/z 888) (Figure 4c). Such $[(NCN)PtPt(NCN)]^+$ species is not detected in the absence of light irradiation. On the basis of the well-documented photochemical Pt-C bond homolysis reactions in Pt compounds to afford Pt radicals,[68] its formation is attributed to homolytic cleavage of the alkynyl ligand to yield the radical (NCN)Pt· that is readily dimerized to [(NCN)PtPt(NCN)]. Both neutral (NCN)Pt· and [(NCN)PtPt(NCN)] species could be inferred from the ESI mass spectrum as their corresponding oxidized $[(NCN)Pt]^+$ (m/z 444) and $[(NCN)PtPt(NCN)]^+$ (m/z 888) homologues. These experiments suggest the involvement of Pt radical species in photohydrosilylation in a similar way to that proposed for the hydrosilylation reactions using $(\eta^5\text{-}C_5H_4CH_3)Pt^{IV}(CH_3)_3$ as a photosensitizer.[44] Further evidence of radicals during the photohydrosilylation reaction was obtained by the addition of stochiometric quantities of galvinoxyl under photocatalytic conditions (Table 4). This test inhibited the reaction and only 20% yield vinylsilanes were produced in contrast to the 99% in the absence of the radical scavenger. These results provide further evidence of radical formation during photohydrosilylation.

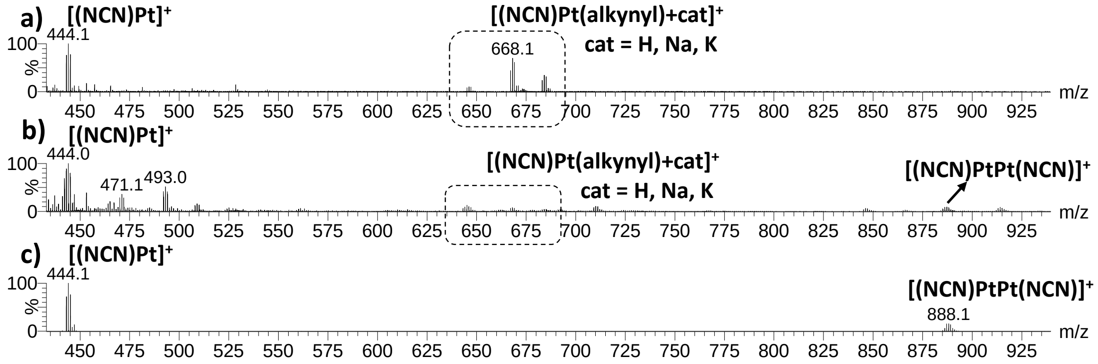

Figure 4 ESI mass spectra of a) methanol solutions of **II** (1 x 10^{-6} M); b) methanol solutions of the catalytic reaction after 2h of light irradiation (diluted to reach 1 x 10^{-6} M concentration based on the initial amount of **II**) and c) methanol solutions of **II** after light irradiation in the absence of substrates.

Table 4. Trapping experiments

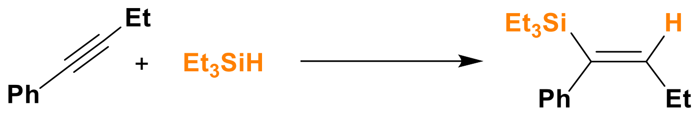

Entry	Trapping agent	Conv (%) Thermal	Conv (%) Photo
1	-	99	99
2	Galvinoxyl	98	20
3	$[CPh_3][BF_4]$	4	11

Standard conditions as described previously with the addition of galvinoxyl (0.6 mmol, 2 eq.) or tritylium tetrafluoroborate (0.03 mmol, 0.1 eq.). Galvinoxyl is a radical scavenger and tritylium tetrafluoroborate ($[CPh_3][BF_4]$) is a hydride scavenger.

Based on the above observations, a plausible mechanism for the visible-light-promoted hydrosilylation of alkynes is proposed (Figure 5). First, complex **I** (or **II**) absorbs blue light forming the triplet state excited species [(NCN)PtL]* (L = Cl or alkynyl) highlighting the role of platinum complexes as photosensitizers. Following the homolytic splitting of the Pt-L bond, the [(NCN)Pt]· radical subsequently abstracts a hydrogen atom from the Si-H bond to generate a silyl radical along with the formation of the hydride complex [(NCN)PtH] through a hydrogen atom transfer (HAT) process. This step is analogous to that proposed for the photohydrosilylation catalysed by $(CO)_5Mn$· radical.[30,31] We hypothesize that a [(NCN)PtH] species might be generated during the reaction and be part of the catalytic cycle; however, we did not succeed at detecting Pt-hydride species experimentally most likely due to its fleeting nature and rapid conversion at the high catalyst load used to detect reaction intermediates.[3] Support to this hypothesis was obtained from experiments of the catalytic reaction in the presence of catalytic amounts of trityl tetrafluoroborate, which is a hydride abstractor.[69] Addition of $[CPh_3][BF_4]$ to the catalytic reaction completely inhibited the reaction providing an indirect evidence of platinum hydrides as intermediates (Table 4). Finally, the addition of the silyl radical to the alkyne delivers radical vinyl species, which undergo another HAT process to yield the desired hydrosilylation products. Herein we have demonstrated that pincer platinum complexes play a dual role in the photohydrosilylation of alkynes, on one hand harvest visible light and on the other hand participate in the bond-breaking/bond forming catalytic transformations thorough HAT type processes.

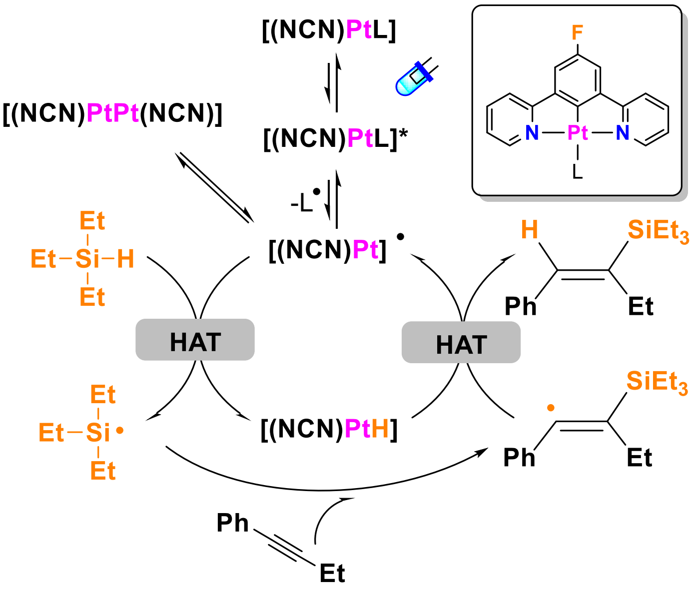

Figure 5 Plausible mechanism for photohydrosilylation mediated by (NCN)Pt complexes.

Deuterium labelling experiments in photohydrosilylation of 1-phenyl-1-butyne and Et_3SiD using complex **II** shows the incorporation of deuterium only at the vinylic positions of the a and b additions as confirmed by ^1H NMR spectroscopy (Figure S33). We have observed an inversed kinetic isotope effect (IKIE) of 0.9. This small value for a primary isotope effect indicates that Si-H cleavage is not involved in the slowest step and supports a preequilibrium before the rate-determining step which further supports the mechanism proposal. In addition, deuterium labelling experiments under thermal conditions were completely different. We observed a normal kinetic isotope effect (KIE) of 1.2 (Figure S34). These differences evidence a different reaction mechanism under photo or thermal conditions. The reaction monitoring of the species formed during the thermal reaction (hydrosilylation of 1-phenyl-1-butyne with dimethylphenylsilane mediated by **II**) was also investigated by ESI-MS. Low intensity high-nuclearity aggregates bearing silane and alkyne bound substrates were evidenced based on ESI-MS. Peak assignment was done on the basis of their characteristic isotopic pattern (Figure S39). Such species are indicative that oxidative addition of R_3SiH on such larger aggregates has occurred most likely preceded by the reduction of metal core by a sacrificial amount of silane substrate. Species formulated as the dimers $[[(NCN)Pt]_2H]^+$ (m/z 889.1), the alkyne-coordinated species, namely $[((NCN)Pt)_2(H)(C_{10}H_{10})]^+$ (m/z 1020.1) $[((NCN)Pt)_2(Cl)(C_{10}H_{10})]^+$ (m/z 1055.1), $[((NCN)Pt)_2((CH_3)_2PhSi)(C_{10}H_{10})]^+$ (m/z 1151.3) and the trimer $[((NCN)Pt)_3H_2]^+$ (m /z 1334.2) were observed in the ESI mass spectrum recorded along the catalytic thermal reaction (Figure 6). We are aware that the coexistence of mononuclear and larger aggregates bearing silyl or alkyne makes challenging to propose the exact nature of the Pt active species and its mechanism of action. In this sense, Pt dimers[70] or Pt–Si–H clusters of 3–5 atoms were recently proposed as key catalyst in the Pt-catalysed hydrosilylation of alkynes.[71] Nonetheless, the operation of a mechanism that involves organometallic intermediates is clearly evidenced. Consistent with this hypothesis, the addition of stochiometric quantities of galvinoxyl does not inhibit the reaction.

Similar yield to the control experiment and identical regio- and stereoselectivity was observed in the absence/presence of galvinoxyl (Table 4). However, the addition of [CPh_3][BF_4] to the catalytic reaction completely inhibited the reaction consistent with the presence of platinum hydride species. These results support a reaction mechanism under thermal conditions that involve organometallic platinum hydride species analogous to the classical Chalk-Harrod mechanisms.

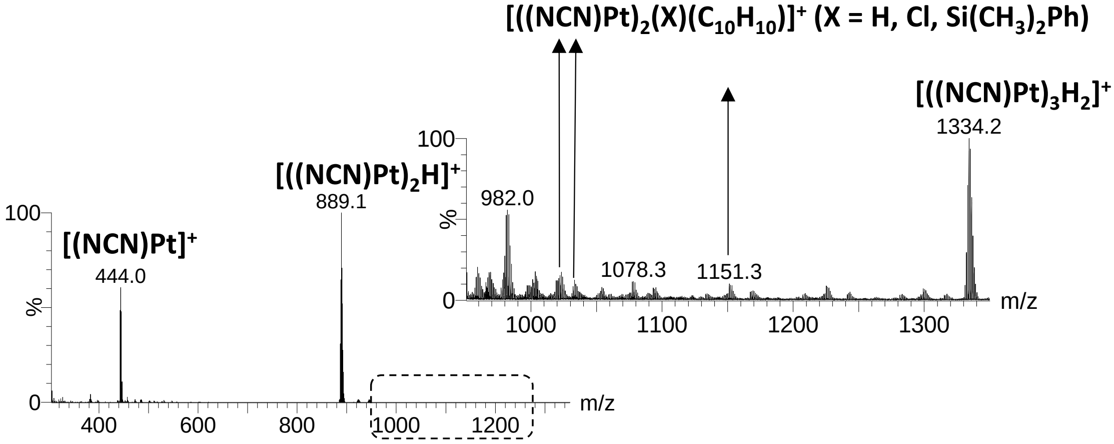

Figure 6 ESI mass spectrum of an aliquot taken from the catalytic reaction using **I** and 1-phenyl-1-butyne with dimethylphenylsilane after 2h under thermal conditions, diluted with methanol (1 x 10^{-6} M with respect to the initial amount of catalyst **I**). The inset shows the expanded region in the m/z 950-1350 range where the organometallic/silane Pt species are observed.

4. CONCLUSIONS

We have shown that (NCN)Pt(II) complexes **I** and **II** constitute efficient visible light-induced transition metal catalysis (in which the metal complex itself serves as both photosensitizer and catalyst enabling species) capable to perform the hydrosilylation of a series of internal and terminal alkynes at ambient temperature. Reasonable product yields can be also obtained in the absence of light but operate at high temperatures (typically 80 °C). Mechanistically, the observed light-induced vs thermal-induced hydrosilylation proceeds through either a radical-mediated pathway or that involving organometallic silane complexes, respectively. The catalytic use of mononuclear **I** and **II** under thermal conditions afford exclusively the E-products with moderate α/β regioselectivity for a series of internal alkynes. Selectivity can be enhanced by using the same systems under visible light irradiation under milder conditions, thus making these conditions compatible with thermally unstable substrates. In the case of terminal alkynes, both procedures displayed identical trends except that light-induced catalysis enabled the formation of Z-products in a reversed stereoselectivity. A prominent propensity towards Z selectivity is also observed using the closely related $(CO)_5Mn\cdot$ radical as visible light-induced transition metal catalysis. Such a moderate control on regio- and stereodivergency highlights a unique feature of the investigated pincer-type Pt complexes in the context of regiodivergent catalysis which is most often triggered through the judicious choice of the metal or the ligands in the catalytic system. The present Pt catalytic system provides different products from common starting materials by switching light vs- thermal-mediated hydrosilylation and adds to the still rare members of regiodivergent catalysis achieved photochemically. Moreover, these NCN ligands may combine a wide spectrum of donor properties with steric flexibility, easily modulable in the fine-tuning of the photocatalytic properties, and can easily be prepared via several well-established methods. Further improvements through the rational catalyst design are expected to address the regioselective issues raised.

Supporting Information

Photoreactor set-up, spectroscopic characterization of products and selectivity assignments, further details of mechanistic studies (experimental procedures, NMR characterization, ESI-MS and trapping experiments).

Acknowledgements

Thanks to PID2021-126071OB-C22 and PID2019-104121GB-I00 funded by MICIN/AEI/10.13039/501100011033/ FEDER "Una manera de hacer Europa". Generalitat Valenciana (PROMETEU/2020/028) and Universitat Jaume I (UJI-B2022-23). L. I-I. thanks MICIN for grant (FPU20/04385). The authors thank 'Servei Central d'Instrumentació Científica (SCIC) de la Universitat Jaume I'.

AUTHOR INFORMATION

Corresponding authors

Jose A. Mata - Institute of Advanced Materials (INAM), Centro de Innovación en Química Avanzada (ORFEO-CINQA), Universitat Jaume I, Avda. Sos Baynat s/n, 12071, Castellón (Spain). E-mail: jmata@uji.es

Laura Rodríguez - Departament de Química Inorgànica i Orgànica, Secció de Química Inorgànica, Universitat de Barcelona, E-08028 Barcelona (Spain). Institut de Nanociència i Nanotecnologia (IN2UB), Universitat de Barcelona, 08028, Barcelona (Spain).

Authors ORCID

Laura Ibáñez-Ibáñez, laibanez@uji.es	ORCID: 0000-0002-6467-1255
Ariadna Lázaro, ariadna.lazaro@qi.ub.edu	ORCID: 0000-0003-4064-3257
Carmen Mejuto Nieblas, mejuto@uji.es	ORCID: 0000-0002-4432-5697
Margarita Crespo, margarita.crespo@qi.ub.es	ORCID: 0000-0002-7086-9751
Cristian Vicent, barrera@uji.es	ORCID: 0000-0002-8288-0384
Laura Rodríguez, laura.rodriguez@qi.ub.es	ORCID: 0000-0003-1289-1587
Jose A. Mata, jmata@uji.es	ORCID: 0000-0001-9310-2783

Author Contributions

The manuscript was written through contributions of all authors. All authors have given approval to the final version of the manuscript.

Funding sources

MICIU/AEI/FEDER (PID2021-126071OB-C22 and PID2019-104121GB-I00). Universitat Jaume I (UJI-B2022-23). Generalitat Valenciana (PROMETEU/2020/028).

Notes

The authors declare no competing financial interests.

Abbreviations

HAT, Hydrogen Atom transfer; ESI-MS, Electrospray Ionization Mass Spectrometry

Social Media

Institute Twitter username: @inam_uji, @QuimicaUB

Researcher Twitter username: @jose_mata_uji, @lrraurell

REFERENCES

[1] R. Hofmann, M. Vlatković, F. Wiesbrock, Fifty Years of Hydrosilylation in Polymer Science: A Review of Current Trends of Low-Cost Transition-Metal and Metal-Free Catalysts, Non-Thermally Triggered Hydrosilylation Reactions, and Industrial Applications, Polymers. 9 (2017) 534–571. https://doi.org/10.3390/polym9100534.

[2] D. Troegel, J. Stohrer, Recent advances and actual challenges in late transition metal catalyzed hydrosilylation of olefins from an industrial point of view, Coord. Chem. Rev. 255 (2011) 1440–1459. https://doi.org/10.1016/j.ccr.2010.12.025.

[3] Y. Nakajima, S. Shimada, Hydrosilylation reaction of olefins: recent advances and perspectives, RSC Adv. 5 (2015) 20603–20616. https://doi.org/10.1039/C4RA17281G.

[4] A. Zanardi, E. Peris, J. a. Mata, Alkenyl-functionalized NHC iridium-based catalysts for hydrosilylation, New J. Chem. 32 (2008) 120–126. https://doi.org/10.1039/b707280e.

[5] T.K. Meister, K. Riener, P. Gigler, J. Stohrer, W.A. Herrmann, F.E. Kühn, Platinum Catalysis Revisited—Unraveling Principles of Catalytic Olefin Hydrosilylation, ACS Catal. 6 (2016) 1274–1284. https://doi.org/10.1021/acscatal.5b02624.

[6] R.Y. Lukin, A.M. Kuchkaev, A. V. Sukhov, G.E. Bekmukhamedov, D.G. Yakhvarov, Platinum-Catalyzed Hydrosilylation in Polymer Chemistry, Polymers. 12 (2020) 2174–2196. https://doi.org/10.3390/polym12102174.

[7] M. Pagliaro, R. Ciriminna, V. Pandarus, F. Béland, Platinum-Based Heterogeneously Catalyzed Hydrosilylation, European J. Org. Chem. 2013 (2013) 6227–6235. https://doi.org/10.1002/ejoc.201300290.

[8] L.N. Lewis, J. Stein, Y. Gao, R.E. Colborn, G. Hutchins, Platinum catalysts used in the silicone industry, Platin. Met. Rev. 41 (1997) 66–75.

[9] A. Mollar-Cuni, P. Borja, S. Martin, G. Guisado-Barrios, J.A. Mata, A Platinum Molecular Complex Immobilised on the Surface of Graphene as Active Catalyst in Alkyne Hydrosilylation, Eur. J. Inorg. Chem. 2020 (2020) 4254–4262. https://doi.org/10.1002/ejic.202000356.

[10] B. Marciniec, Catalysis by transition metal complexes of alkene silylation–recent progress and mechanistic implications, Coord. Chem. Rev. 249 (2005) 2374–2390. https://doi.org/10.1016/j.ccr.2005.02.025.

[11] J. Stein, L.N. Lewis, Y. Gao, R.A. Scott, In Situ Determination of the Active Catalyst in Hydrosilylation Reactions Using Highly Reactive Pt(0) Catalyst Precursors, J. Am. Chem. Soc. 121 (1999) 3693–3703. https://doi.org/10.1021/ja9825377.

[12] P. Gigler, M. Drees, K. Riener, B. Bechlars, W.A. Herrmann, F.E. Kühn, Mechanistic insights into the hydrosilylation of allyl compounds – Evidence for different coexisting reaction pathways, J. Catal. 295 (2012) 1–14. https://doi.org/10.1016/j.jcat.2012.06.006.

[13] A.J. Chalk, J.F. Harrod, Homogeneous Catalysis. II. The Mechanism of the Hydrosilation of Olefins Catalyzed by Group VIII Metal Complexes 1, J. Am. Chem. Soc. 87 (1965) 16–21. https://doi.org/10.1021/ja01079a004.

[14] C. Chatgilialoglu, Structural and Chemical Properties of Silyl Radicals, Chem. Rev. 95 (1995) 1229–1251. https://doi.org/10.1021/cr00037a005.

[15] X. Shang, Z.-Q. Liu, Recent developments in free-radical-promoted C–Si formation via selective C–H/Si–H functionalization, Org. Biomol. Chem. 14 (2016) 7829–7831. https://doi.org/10.1039/C6OB00797J.

[16] W.-B. Liu, D.P. Schuman, Y.-F. Yang, A.A. Toutov, Y. Liang, H.F.T. Klare, N. Nesnas, M. Oestreich, D.G. Blackmond, S.C. Virgil, S. Banerjee, R.N. Zare, R.H. Grubbs, K.N. Houk, B.M. Stoltz, Potassium tert -Butoxide-Catalyzed Dehydrogenative C–H Silylation of Heteroaromatics: A Combined Experimental and Computational Mechanistic Study, J. Am. Chem. Soc. 139 (2017) 6867–6879. https://doi.org/10.1021/jacs.6b13031.

[17] S.B. Cahoon, T.P. Yoon, 1.5 Photochemistry and Radical Generation: Approaches in Mechanism Elucidation, in: Free Radicals Fundam. Appl. Org. Synth. 1, Georg Thieme Verlag KG, Stuttgart, 2021. https://doi.org/10.1055/sos-SD-234-00064.

[18] N. Kvasovs, V. Gevorgyan, Contemporary methods for generation of aryl radicals, Chem. Soc. Rev. 50 (2021) 2244–2259. https://doi.org/10.1039/D0CS00589D.

[19] J. Li, J. Wu, Recent Developments in the Photo-Mediated Generation of Silyl Radicals and Their Application in Organic Synthesis, ChemPhotoChem. 2 (2018) 839–846. https://doi.org/10.1002/cptc.201800110.

[20] S. Ghosh, D. Lai, A. Hajra, Visible-light-induced silylation: an update, Org. Biomol. Chem. 19 (2021) 2399–2415. https://doi.org/10.1039/d1ob00082a.

[21] L.-Q. Ren, N. Li, J. Ke, C. He, Recent advances in photo- and electro-enabled radical silylation, Org. Chem. Front. 9 (2022) 6400–6415. https://doi.org/10.1039/D2QO01387H.

[22] H. Cao, X. Tang, H. Tang, Y. Yuan, J. Wu, Photoinduced intermolecular hydrogen atom transfer reactions in organic synthesis, Chem Catal. 1 (2021) 523–598. https://doi.org/10.1016/j.checat.2021.04.008.

[23] K.P.S. Cheung, S. Sarkar, V. Gevorgyan, Visible Light-Induced Transition Metal Catalysis, Chem. Rev. 122 (2022) 1543–1625. https://doi.org/10.1021/acs.chemrev.1c00403.

[24] R. Kancherla, K. Muralirajan, A. Sagadevan, M. Rueping, Visible Light-Induced Excited-State Transition-Metal Catalysis, Trends Chem. 1 (2019) 510–523. https://doi.org/10.1016/j.trechm.2019.03.012.

[25] M. Parasram, V. Gevorgyan, Visible light-induced transition metal-catalyzed transformations: beyond conventional photosensitizers, Chem. Soc. Rev. 46 (2017) 6227–6240. https://doi.org/10.1039/C7CS00226B.

[26] W.-M. Cheng, R. Shang, Transition Metal-Catalyzed Organic Reactions under Visible Light: Recent Developments and Future Perspectives, ACS Catal. 10 (2020) 9170–9196. https://doi.org/10.1021/acscatal.0c01979.

[27] N. Hoffmann, Homogeneous Photocatalytic Reactions with Organometallic and Coordination Compounds-Perspectives for Sustainable Chemistry, ChemSusChem. 5 (2012) 352–371. https://doi.org/10.1002/cssc.201100286.

[28] C. Mejuto, L. Ibáñez-Ibáñez, G. Guisado-Barrios, J.A. Mata, Visible-Light-Promoted Iridium(III)-Catalyzed Acceptorless Dehydrogenation of N-Heterocycles at Room Temperature, ACS Catal. 12 (2022) 6238–6245. https://doi.org/10.1021/acscatal.2c01224.

[29] H. Qrareya, D. Dondi, D. Ravelli, M. Fagnoni, Decatungstate-Photocatalyzed Si−H/C−H Activation in Silyl Hydrides: Hydrosilylation of Electron-Poor Alkenes, ChemCatChem. 7 (2015) 3350–3357. https://doi.org/10.1002/cctc.201500562.

[30] H. Liang, Y.-X. Ji, R.-H. Wang, Z.-H. Zhang, B. Zhang, Visible-Light-Initiated Manganese-Catalyzed E -Selective Hydrosilylation and Hydrogermylation of Alkynes, Org. Lett. 21 (2019) 2750–2754. https://doi.org/10.1021/acs.orglett.9b00701.

[31] X. Yang, C. Wang, Dichotomy of Manganese Catalysis via Organometallic or Radical Mechanism: Stereodivergent Hydrosilylation of Alkynes, Angew. Chem. Int. Ed. 57 (2018) 923–928. https://doi.org/10.1002/anie.201710206.

[32] A. V. Radchenko, F. Ganachaud, Photocatalyzed Hydrosilylation in Silicone Chemistry, Ind. Eng. Chem. Res. 61 (2022) 7679–7698. https://doi.org/10.1021/acs.iecr.2c01015.

[33] A.L. Prignano, W.C. Trogler, Silica-supported bis(trialkylphosphine)platinum oxalates. Photogenerated catalysts for hydrosilylation of olefins, J. Am. Chem. Soc. 109 (1987) 3586–3595. https://doi.org/10.1021/ja00246a015.

[34] R.S. Paonessa, A.L. Prignano, W.C. Trogler, Photochemical generation of bis(phosphine)palladium and bis(phosphine)platinum equivalents, Organometallics. 4 (1985) 647–657. https://doi.org/10.1021/om00123a006.

[35] F.D. Lewis, G.D. Salvi, Platinum(II) Bis(.beta.-diketonates) as Photoactivated Hydrosilation Catalysts, Inorg. Chem. 34 (1995) 3182–3189. https://doi.org/10.1021/ic00116a008.

[36] T. Mayer, D. Burget, G. Mignani, J.P. Fouassier, Photohydrosilylation reaction of silicone polymers. Platinum-based photocatalysts: Trimethyl(β-dicarbonyl) platinum(IV)

complexes, J. Polym. Sci. Part A Polym. Chem. 34 (1996) 3141–3146. https://doi.org/10.1002/(sici)1099-0518(19961115)34:15<3141::aid-pola5>3.0.co;2-%23.

[37] B.E. Fry, D.C. Neckers, Rapid Photoactivated Hydrosilation Polymerization of Vinyldimethylsilane, Macromolecules. 29 (1996) 5306–5312. https://doi.org/10.1021/ma960194w.

[38] B.E. Fry, A. Guo, D.C. Neckers, Photoactivated hydrosilation curing of a ceramic precursor: Crosslinking and pyrolysis of branched oligo[(methylsilylene) methylene], J. Organomet. Chem. 538 (1997) 151–161. https://doi.org/10.1016/S0022-328X(97)00042-9.

[39] G. Zhang, J. Kong, X. Fan, X. Li, W. Tian, M. Huang, UV&hyphen;activated hydrosilylation: a facile approach for synthesis of hyperbranched polycarbosilanes, Appl. Organomet. Chem. 23 (2009) 277–282. https://doi.org/10.1002/aoc.1511.

[40] S. Marchi, M. Sangermano, D. Ligorio, P. Meier, X. Kornmann, Impressive Rate Raise of the Hydrosilation Reaction Through UV-Activation: Energy and Time Saving, Macromol. Mater. Eng. 301 (2016) 610–613. https://doi.org/10.1002/mame.201500413.

[41] A. Guo, B.E. Fry, D.C. Neckers, Highly Active Visible-Light Photocatalysts for Curing a Ceramic Precursor 1, Chem. Mater. 10 (1998) 531–536. https://doi.org/10.1021/cm970518a.

[42] J.C. Gee, B.A. Fuller, H.M. Lockett, G. Sedghi, C.M. Robertson, K. V. Luzyanin, Visible light accelerated hydrosilylation of alkynes using platinum-[acyclic diaminocarbene] photocatalysts, Chem. Commun. 54 (2018) 9450–9453. https://doi.org/10.1039/c8cc04287j.

[43] M. V. Kashina, K. V. Luzyanin, E.A. Katlenok, A.S. Novikov, M.A. Kinzhalov, Experimental and computational tuning of metalla-N-heterocyclic carbenes at palladium(ii) and platinum(ii) centers, Dalt. Trans. 51 (2022) 6718–6734. https://doi.org/10.1039/D2DT00252C.

[44] V. Jakubek, A.J. Lees, Solution : A Highly Efficient Organometallic Photoinitiator for Hydrosilylation, Inorg. Chem. 43 (2004) 6869–6871.

[45] S. Marchi, M. Sangermano, P. Meier, X. Kornmann, Visible light-activated hydrosilation reaction, J. Photochem. Photobiol. A Chem. 303–304 (2015) 86–90. https://doi.org/10.1016/j.jphotochem.2015.02.013.

[46] A. Lázaro, R. Bosque, J.S. Ward, K. Rissanen, M. Crespo, L. Rodríguez, Toward Near-Infrared Emission in Pt(II)-Cyclometallated Compounds: From Excimers’ Formation to Aggregation-Induced Emission, Inorg. Chem. 62 (2023) 2000–2012. https://doi.org/10.1021/acs.inorgchem.2c03490.

[47] V.W.-W. Yam, A.S.-Y. Law, Luminescent d8 metal complexes of platinum(II) and gold(III): From photophysics to photofunctional materials and probes, Coord. Chem. Rev. 414 (2020) 213298. https://doi.org/10.1016/j.ccr.2020.213298.

[48] S. Zhao, Y. Zhu, L. Li, V. Guerchais, J. Boixel, K.M.-C. Wong, The switchable phosphorescence and delayed fluorescence of a new rhodamine-like dye through allenylidene formation in a cyclometallated platinum(II) system, Chem. Sci. 12 (2021) 11056–11064. https://doi.org/10.1039/D1SC02787E.

[49] V.W.-W. Yam, V.K.-M. Au, S.Y.-L. Leung, Light-Emitting Self-Assembled Materials Based on d 8 and d 10 Transition Metal Complexes, Chem. Rev. 115 (2015) 7589–7728.

https://doi.org/10.1021/acs.chemrev.5b00074.

[50] A. Lázaro, C. Balcells, J. Quirante, J. Badia, L. Baldomà, J.S. Ward, K. Rissanen, M. Font-Bardia, L. Rodríguez, M. Crespo, M. Cascante, Luminescent Pt II and Pt IV Platinacycles with Anticancer Activity Against Multiplatinum-Resistant Metastatic CRC and CRPC Cell Models, Chem. – A Eur. J. 26 (2020) 1947–1952. https://doi.org/10.1002/chem.201905325.

[51] M. Martínez-Junquera, R. Lara, E. Lalinde, M.T. Moreno, Isomerism, aggregation-induced emission and mechanochromism of isocyanide cycloplatinated(II) complexes, J. Mater. Chem. C. 8 (2020) 7221–7233. https://doi.org/10.1039/D0TC01163K.

[52] M. Hruzd, S. Gauthier, J. Boixel, S. Kahlal, N. le Poul, J.-Y. Saillard, S. Achelle, F.R. Guen, N^N^C platinum (II) complexes based on phenyl-pyridin-2-ylpyrimidine ligands: synthesis, electrochemical and photophysical properties, Dye. Pigment. 194 (2021) 109622. https://doi.org/10.1016/j.dyepig.2021.109622.

[53] A.K.-W. Chan, M. Ng, Y.-C. Wong, M.-Y. Chan, W.-T. Wong, V.W.-W. Yam, Synthesis and Characterization of Luminescent Cyclometalated Platinum(II) Complexes with Tunable Emissive Colors and Studies of Their Application in Organic Memories and Organic Light-Emitting Devices, J. Am. Chem. Soc. 139 (2017) 10750–10761. https://doi.org/10.1021/jacs.7b04952.

[54] T. Von Grotthuss, Auszug aus vier Abhandlungen Physikalisch-chemischen Inhalts, Ann. Der Phys. Und Der Phys. Chemie. 61 (1819) 50–74. https://doi.org/10.1002/andp.18190610105.

[55] J.W. Draper, XXX. On some analogies between the phænomena of the chemical rays, and those of radiant heat, London, Edinburgh, Dublin Philos. Mag. J. Sci. 19 (1841) 195–210. https://doi.org/10.1080/14786444108650398.

[56] F. Nisic, A. Colombo, C. Dragonetti, D. Roberto, A. Valore, J.M. Malicka, M. Cocchi, G.R. Freeman, J.A.G. Williams, Platinum(ii) complexes with cyclometallated 5-π-delocalized-donor-1,3-di(2-pyridyl)benzene ligands as efficient phosphors for NIR-OLEDs, J. Mater. Chem. C. 2 (2014) 1791–1800. https://doi.org/10.1039/c3tc32086c.

[57] A. Lázaro, C. Cunha, R. Bosque, J. Pina, J.S. Ward, K.-N. Truong, K. Rissanen, J.C. Lima, M. Crespo, J.S. Seixas de Melo, L. Rodríguez, Room-Temperature Phosphorescence and Efficient Singlet Oxygen Production by Cyclometalated Pt(II) Complexes with Aromatic Alkynyl Ligands, Inorg. Chem. 59 (2020) 8220–8230. https://doi.org/10.1021/acs.inorgchem.0c00577.

[58] B. Fang, Y. Zhu, L. Hu, Y. Shen, G. Jiang, Q. Zhang, X. Tian, S. Li, H. Zhou, J. Wu, Y. Tian, Series of C^N^C Cyclometalated Pt(II) Complexes: Synthesis, Crystal Structures, and Nonlinear Optical Properties in the Near-Infrared Region, Inorg. Chem. 57 (2018) 14134–14143. https://doi.org/10.1021/acs.inorgchem.8b01967.

[59] S.I. Faßbender, J.J. Molloy, C. Mück-Lichtenfeld, R. Gilmour, Geometric E → Z Isomerisation of Alkenyl Silanes by Selective Energy Transfer Catalysis: Stereodivergent Synthesis of Triarylethylenes via a Formal anti -Metallometallation, Angew. Chem. Int. Ed. 58 (2019) 18619–18626. https://doi.org/10.1002/anie.201910169.

[60] J. Burés, A Simple Graphical Method to Determine the Order in Catalyst, Angew. Chem. Int. Ed. 55 (2016) 2028–2031. https://doi.org/10.1002/anie.201508983.

[61] L.P.E. Yunker, R.L. Stoddard, J.S. McIndoe, Practical approaches to the ESI-MS

analysis of catalytic reactions, J. Mass Spectrom. 49 (2014) 1–8. https://doi.org/10.1002/jms.3303.

[62] K.L. Vikse, Z. Ahmadi, J. Scott McIndoe, The application of electrospray ionization mass spectrometry to homogeneous catalysis, Coord. Chem. Rev. 279 (2014) 96–114. https://doi.org/10.1016/j.ccr.2014.06.012.

[63] J. Mehara, J. Roithová, Identifying reactive intermediates by mass spectrometry, Chem. Sci. 11 (2020) 11960–11972. https://doi.org/10.1039/D0SC04754F.

[64] A. Mollar-Cuni, L. Ibáñez-Ibáñez, G. Guisado-Barrios, J.A. Mata, C. Vicent, Introducing Ion Mobility Mass Spectrometry to Identify Site-Selective C-H Bond Activation in N-Heterocyclic Carbene Metal Complexes, J. Am. Soc. Mass Spectrom. 33 (2022) 2291–2300. https://doi.org/10.1021/jasms.2c00257.

[65] M.O. Rodrigues, M.N. Eberlin, B.A.D. Neto, How and Why to Investigate Multicomponent Reactions Mechanisms? A Critical Review, Chem. Rec. 21 (2021) 2762–2781. https://doi.org/10.1002/tcr.202000165.

[66] J. V. Burykina, V.P. Ananikov, Studying Photochemical Transformations using Electrospray Ionization Mass Spectrometry (ESI-MS), ChemPhotoChem. 7 (2023) 3–7. https://doi.org/10.1002/cptc.202200175.

[67] Y. Li, I. Sorribes, C. Vicent, K. Junge, M. Beller, Convenient Reductive Methylation of Amines with Carbonates at Room Temperature, Chem. - A Eur. J. 21 (2015) 16759–16763. https://doi.org/10.1002/chem.201502917.

[68] J. van Slageren, A. Klein, S. Záliš, Ligand-to-ligand charge transfer states and photochemical bond homolysis in metal□carbon bonded platinum complexes, Coord. Chem. Rev. 230 (2002) 193–211. https://doi.org/10.1016/S0010-8545(02)00092-9.

[69] S.R. Bahr, P. Boudjouk, Trityl tetrakis[3,5-bis(trifluoromethyl)phenyl]borate: a new hydride abstraction reagent, J. Org. Chem. 57 (1992) 5545–5547. https://doi.org/10.1021/jo00046a048.

[70] A.K. Roy, R.B. Taylor, The First Alkene−Platinum−Silyl Complexes: Lifting the Hydrosilation Mechanism Shroud with Long-Lived Precatalytic Intermediates and True Pt Catalysts, J. Am. Chem. Soc. 124 (2002) 9510–9524. https://doi.org/10.1021/ja0127335.

[71] M. Rivero-Crespo, J. Oliver-Meseguer, K. Kapłońska, P. Kuśtrowski, E. Pardo, J.P. Cerón-Carrasco, A. Leyva-Pérez, Cyclic metal(oid) clusters control platinum-catalysed hydrosilylation reactions: from soluble to zeolite and MOF catalysts, Chem. Sci. 11 (2020) 8113–8124. https://doi.org/10.1039/D0SC02391D.

TOC

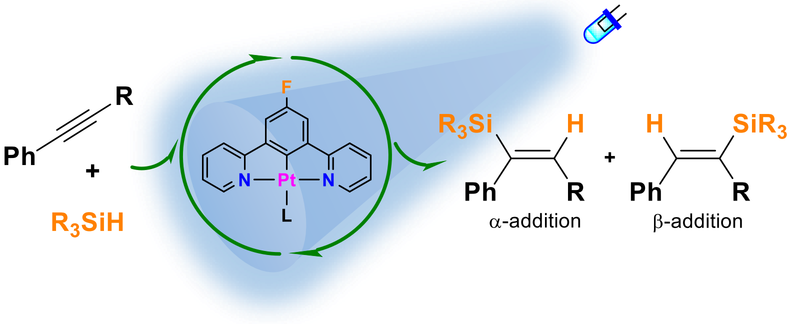

Increasing the efficiency of hydrosilylation assisted by visible-light. Catalytic properties and reaction mechanism with the formation of radicals where the platinum complexes play a dual role as harvesting light species and enabling bond breaking/forming transformations.